Simultaneous Measurement of Photoacoustic and Excitation Spectra for the Evaluation of Quantum Efficiencies of Uranium-mica Type Compounds

Yoshinori SUGITANI* and Kenji KATO†

Institute of Chemistry, The University of Tsukuba, Sakura-mura, Ibaraki 305

(Received April 3, 1979)

A new method of estimating the absolute quantum efficiency of a phosphor material based on the simultaneous measurement of photoacoustic and fluorescent excitation spectra is presented. The method is distinguishable from previous methods in that a reference material is not required. The method has been successfully applied to uranium-mica compounds. The transition rate constants for the radiative and non-radiative processes have been obtained on the basis of the quantum efficiency and fluorescence life time data.

The determination of the absolute quantum efficiency of fluorescence may be achieved either by determination of a defined fraction of the fluorescent radiation, or by the measurement of the complementary part of the non-radiative process by calorimetry.[1] The former optical method appears to be more popular due to the relatively sensitive detection of the fluorescent radiation, which is more sensitive than thermal detection. Electronic units and components are also readily available. The actual determination of quantum efficiency, however, consists of various processes and the necessary corrections, and results are generally of low accuracy.

Determination with the aid of photoacoustic spectrometry belongs to the latter case. Lahmann and Ludewig[2] compared the photoacoustic signal of the sample solution of rhodamine 6G with that of a reference solution of $K_2Cr_2O_7$ which is nonfluorescent but has comparable absorption coefficients. Adams *et al.*[3] determined the quantum efficiency of quinine bisulfate in aqueous solution utilizing the quenching effect of fluorescence by halide ions.

A study of photoacoustic spectra combined with fluorescence spectra enables the flow of the relaxed energy passing through both processes, radiative and non-radiative, to be traced.[4] Simultaneous detection of the photoacoustic and excitation signals as a function of the wave length of the exciting light enables the determination of the absolute quantum efficiencies of fluorescence, as discussed on the uranium-mica type compounds in the present study.

Experimental

Apparatus. The system for the simultaneous measurement of photoacoustic and excitation spectra is shown in Fig. 1, where the system for measuring emission spectra and luminescence life times is also shown. The exciting light from the xenon lamp (300 W) is chopped (CHl) at 80 Hz and monochromated at SPl(JASCO, CT-25N) and irradiated on the sample cell (PFC), the details of which are reported in this journal.[5] The photoacoustic signal is detected by a microphone (SONY, Electlet condenser type, FET buffer included, parts number 8-814-196-50) attatched on the cell, amplified at Pl, introduced to a lock-in amplifier L2 (NF Circuit Design Block, LI-574) and recorded on R2. The optical signal is filtered at SP2, detected by a photomultiplier (PM), amplified (P3 and L1) and recorded on R1.

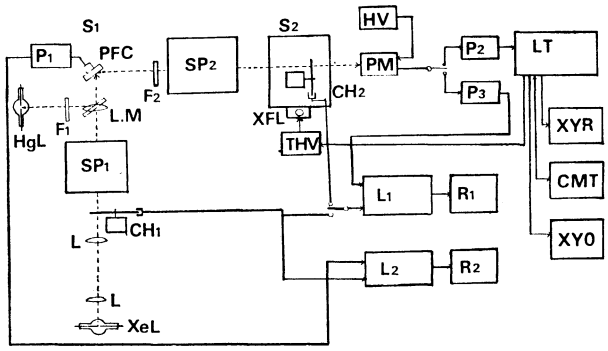

Fig. 1. Block diagram showing the system for simultaneous measurement of photoacoustic and fluorescent excitation spectra. The system for measuring emission spectra and fluorescent life time are also shown. XeL: Xenon arc lamp, L: lenses, CH1 and CH2: light choppers, HgL: mercury lamp, F1 and F2: filters, PFC: sample cell, S1 and S2: sample position, THV: trigger circuit and power supply for xenon flash lamp, XFL: xenon flash lamp, PM: photomultiplier, P1, P2, and P3: preamplifiers, L1 and L2: lock-in amplifiers, R1 and R2: recorders, LT: signal processor unit with a microcomputer, XYR: XY-recorder, CMT: magnetic cassette tape, XYO: XY-oscilloscope, SP1 and SP2: spectrometers.

In the measurement of emission spectra, the sample is irradiated with UV light (365 nm) from a mercury lamp (HgL) and the fluorescent emission is monochromated by the spectrometer SP2 (NIKON, P-250), chopped (CH2), and detected by the photomultiplier PM. With the luminescence life time measurement, the sample specimen is placed in the S2 position instead of the S1 position and, is excited by a xenon flash lamp XFL. The fluorescent signal is detected (PM), amplified (P2), and introduced to the life time measuring system LT, the details of which will be published elsewhere.[6]

All measurements in the present study were taken at room temperature.

Samples. The samples used in the present study are the same as those described previously.[7,8]

Results and Discussion

Procedure for Determining Quantum Efficiency. In a system which is not chemically reactive to visible light

† Present address: National Chemical Laboratory for Industry, 1-1 Yatabe-cho Higashi, Tsukuba-gun, Ibaraki 305.

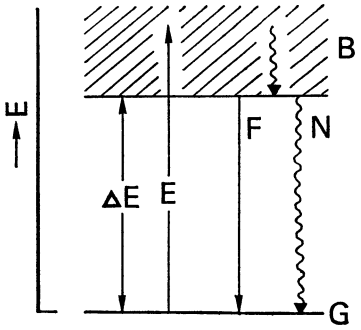

Fig. 2. An energy diagram tentatively given for derivating the relations of quantum efficiency calculation. F: Radiative process, N: non-radiative process.

irradiation, photoacoustic spectrometry provides a complementary system to fluorescent spectrometry which deals with the radiative process. A method of estimating the absolute quantum efficiency of fluorescence Q_F is presented in Fig. 2, based on a simple model of energy diagram where the ground state G and the excited state B of a broad band is given with a separation of ΔE. Assuming the system absorbs light energy E larger than ΔE, the system will release heat energy and will return to the bottom of the band, from which the system will relax to the ground state G by a radiative (F) and/or non-radiative (N) transition. The intensity of the fluorescent emission $I_F(E)$ caused by the excitation of light with energy E is given by

$$I_F(E) = k \cdot \beta(E) \cdot Q_F \cdot I_{EX}(E), \tag{1}$$

where k is a measuring constant, $\beta(E)$ is an absorption coefficient for the light energy E, and $I_{EX}(E)$ is the intensity of the exciting light at energy E. The photoacoustic signal is proportional to the output of thermal energy, which is given as the sum of the excess energy, $E-\Delta E$, and the energy released in the non-radiative process N. Thus the photoacoustic intensity $I_P(E)$ is given by

$$\begin{aligned} I_P(E) &= l \cdot \beta(E) \cdot I_{EX}(E) \cdot [(E-\Delta E)+\Delta E(1-Q_F)] \\ &= l \cdot \beta(E) \cdot I_{EX}(E) \cdot (E-\Delta E \cdot Q_F), \end{aligned} \tag{2}$$

where l is a measuring constant. Supposing that $\beta(E)$ and $I_{EX}(E)$ are taken as invariant, the $I_F(E)$ and $I_P(E)$ will be given as functions of the energy E as in Fig. 3. Taking the ratio of $I_P(E)$ and $I_F(E)$, the $\beta(E)$ and $I_{EX}(E)$ terms vanish giving:

$$\frac{I_P(E)}{I_F(E)} = \frac{1}{k} \cdot \frac{E-\Delta E \cdot Q_F}{Q_F}. \tag{3}$$

The $I_P(E)/I_F(E)$ ratio will be directly related to E as shown in Fig. 3c. Extrapolation leads to an energy of E_0 as in the following;

$$\frac{I_P(E)}{I_F(E)} = 0 = \frac{1}{k} \cdot \frac{E_0-\Delta E \cdot Q_F}{Q_F}, \tag{4}$$

i.e.,

$$E_0 = \Delta E \cdot Q_F. \tag{5}$$

The quantum efficiency will be given as

$$Q_F = E_0/\Delta E. \tag{6}$$

Experimentally, the E_0 value will be obtained as a crossing point on the E axis in the extropolation of the plots of $I_P(E)/I_F(E)$ *versus* E, and the ΔE value will be obtained as the center of the gravity of the emission spectra.

The method of estimating the quantum efficiency presented here is an improvement of those reported to date,[2,3] in that reference materials and quenched samples are not required. In addition, the simultaneous measurement followed by the plotting of intensity ratios of both spectra removes the need for corrections for the power spectrum and the drift of the exciting light.

Quantum Efficiencies of Uranium-micas. A series of uranium-mica type compounds containing uranyl ions as fluorescent centers may be considered as one of those which have an energy diagram similar to that discussed above. Figure 4 shows an energy level diagram for the uranyl(VI) ion based on the paper of Bell and Biggers[9] which appears to be the most widely accepted diagram for uranyl salts. The totally symmetric singlet ground state $^1\Sigma_g^+$ is split into five sublevels due to symmetric

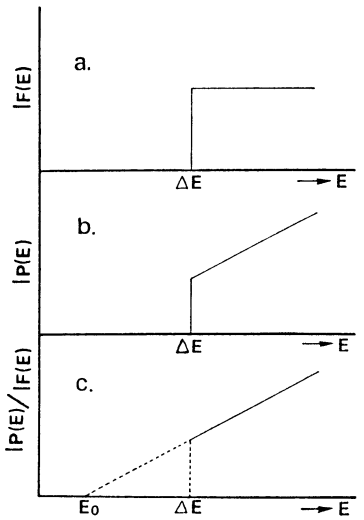

Fig. 3. Expected intensities of fluorescent (a) and photoacoustic (b) output based on the diagram of Fig. 2, and their ratios (c) as a function of the exciting energy E.

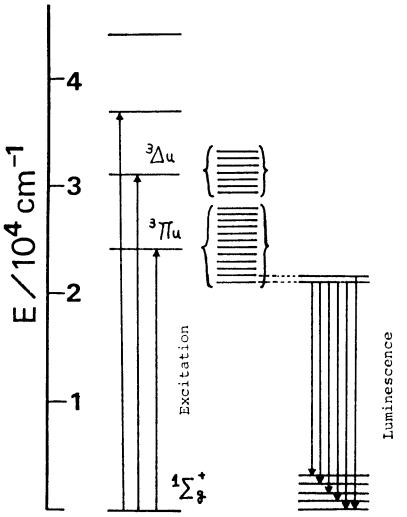

Fig. 4. Energy level diagram showing the transitions of excitation and fluorescent process for uranyl(VI) ion.[9]

stretching in the ground state, while the lowest excited state $^3\Pi_u$ and the second lowest excited state $^3\Delta_u$ are also split into the twelve and seven sublevels, respectively, due to the symmetric stretching in the excited state. The average spacings of the sublevels are approximately 750—860 cm^{-1} depending on the respective sample.[10-12] The luminescence appears to occur from the lowest one or two sublevels to the ground state sublevels showing six emission peaks. The emission peak at the shortest wavelength has a relatively small intensity of about 1/30 of the total intensity suggesting that the contribution to the emission from the second lowest sublevel is negligibly small.

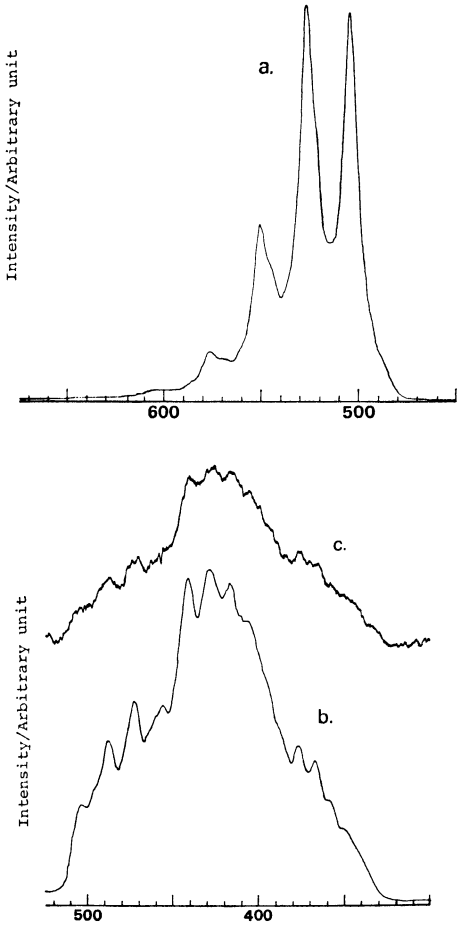

Fig. 5. Fluorescent emission spectra (a), fluorescent excitation spectra (b), and photoacoustic spectra (c) of $Ba(UO_2)_2(PO_4)_2 \cdot nH_2O$. The latter two spectra was simultaneously measured.

The emission spectra of $Ba(UO_2)_2(PO_4)_2 \cdot nH_2O$, one of the prepared uranium-mica samples, are also shown in Fig. 5. The main features of the three spectra for other uranium-mica samples are very similar except for shifts in the peak values of approximately 5 nm in the respective spectra.

Plots of the $I_P(E)/I_F(E)$ ratios *versus* the exciting energy E for the case of Ba-containing uranium-mica samples are given in Fig. 6, where the six points in the lower energy region fall on a straight line giving the experimental E_0 value on the abscissa. The experimental

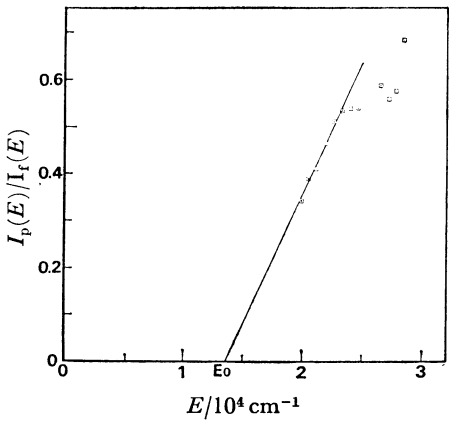

Fig. 6. Plots of the intensity ratios of photoacoustic and fluorescent excitation signals as a function of the exciting energy E.

ΔE value has been tentatively evaluated as 1.92×10^4 cm^{-1} (520 nm) from the peak position of the envelope curve of the emission spectra (Fig. 5a). The value of the quantum efficiency, calculated from Eq. 6 is 0.7. The value of quantum efficiency obtained using similar procedures for the other uranium-micas are given in Table 1. The E_0 value of 1.92×10^4 cm^{-1} has been constantly applied in the estimation of quantum efficiencies of other uranium-micas. The error from this approximation is estimated as $\pm 4\%$. Table 1 includes the fluorescence life times and the transition rate constants which will be discussed later.

In Fig. 6, some of the data in the higher energy region deviate from linearity. This deviation was also found in other unanium micas, where the number of points falling on the line ranges from 4 to 7 out of fifteen.

The reason of the observed deviation appears to be due to the grain size δ of the sample powder. For a photoacoustic signal Ps from a solid sample,[11] Ps varies as a rather complex function of the parameters concerning the sample and/or experimental conditions such as absorption coefficient β, thermal conductivity, grain size δ, chopping frequency ω, *etc.* For the samples studied here the relation between δ and the optical penetration distance, μ, which is defined as $1/\beta$, appears to be responsible for the deviation.

In the situation that μ is larger than δ, the acoustic signal Ps is proportional to β, whereas if μ is comparable to or smaller than δ, the acoustic signal Ps remains constant and independent of β. This indicates that in the energy region with a relatively large β around 400—450 nm, the optical penetration distance μ is equal to or smaller than δ, so that the intensity of the photoacoustic signal will be reduced to some extent, resulting in deviation from linearity. The plots in the higher energy region appear closer to the line than those in the middle energy region which appears to correspond to a lower β value in this region. Samples having a large grain size such as $Mg(UO_2)_2(PO_4)_2 \cdot nH_2O$: Mn (0.03 mol%) show large deviations, while fine grain samples such as $Zn(UO_2)_2(PO_4)_2 \cdot nH_2O$: Cu (0.01 mol%) do not show deviations. It may be concluded

TABLE 1. DATA OF QUANTUM EFFICIENCY Q_F, FLUORESCENCE LIFE TIME τ, AND TRANSITION RATE CONSTANTS k_f AND k_n OF THE RESPECTIVE RADIATIVE AND NON-RADIATIVE PROCESSES, FOR A SERIES OF URANIUM-MICA COMPOUNDS $M(UO_2)_2(XO_4)_2 \cdot nH_2O$

M	X=P				X=As			
	Q_f (%)	τ 10^{-4}s	k_f $10^3 s^{-1}$	k_n $10^3 s^{-1}$	Q_f (%)	τ 10^{-4}s	k_f $10^3 s^{-1}$	k_n $10^3 s^{-1}$
$(H_3O)_2$	0	-	0	-	72	1.4*	5.1*	2.0*
Na_2	86*	2.4	3.6*	0.6*	90	0.82	12.0	1.2
K_2	86	2.8	3.1	0.5	79*	1.0*	7.9*	2.1*
Mg	86	2.8	3.1	0.5	92	1.2	7.7	0.7
Mg:Mn	58	1.7	3.4	2.5	Mn:0.03mol%			
Ca	78*	2.6	3.0*	0.8*	-	1.4*	-	-
Sr	75*	3.4	2.2*	0.7*				
Ba	70	2.8	2.5	1.0	73	1.9	3.9	1.3
Zn:Cu	75*	1.4*	5.4*	1.8*	Cu:0.01mol%			
Zn:Cu	10	1.6*	0.6*	5.6*	Cu:0.1mol%			

* less reliable data

that a sample with a smaller grain size gives greater linearity and thus more reliable results in terms of estimation of the quantum efficiency.

Transition Rate Constants k_f and k_n for the Radiative and Non-radiative Processes. The combination of the values of quantum efficiency Q_F and the fluorescence life time allows the transition rate k_f for the radiative process and k_n for the non-radiative process to be evaluated. The values are related in the following equations;

$$\tau = 1/(k_f + k_n) \quad (7)$$

$$Q_F = k_f/(k_f + k_n), \quad (8)$$

which may be rewritten:

$$k_f = Q_F/\tau \quad (9)$$

$$k_n = (1 - Q_F)/\tau. \quad (10)$$

The results calculated from Eqs. 9 and 10 are given in Table 1. The life time data in Table 1 have been measured in this study, and are slightly different from those previously reported.[8] The difference is considered to be within experimental error so far as the room temperature data are concerned. As seen in Table 1, the phosphate samples have Q_F, k_f, and k_n values of approximately 80%, 3×10^3 s^{-1}, and 0.5—1.0×10^3 s^{-1}, respectively. The arsenate samples have a shorter τ, a slightly larger Q_F, and a larger k_f value than in the phosphate samples. The k_n values are comparable for the phosphate and arsenate samples. This suggests that the fast radiative process (large k_f) makes the life time short for the samples without the quencher ions such as Cr and Mn. The sample with quencher ion $Mg(UO_2)_2(PO_4)_2 \cdot nH_2O$: Mn (0.03 mol%), however, has a shorter τ and lower Q_F leading to a larger value of k_n. It is considered that the effect of the doping ion Mn^{2+} receives part of the excited energy of the UO_2^{2+} ion making the τ value shorter as well as making the Q_F value lower. The effect of the doping ion Cu^{2+}, as seem in Table 1, is to decrease the value of Q_F without changing the life time data. This indicates that the Cu^{2+} ions absorb almost all the excited energy of the nearest UO_2^{2+} ions making the Q_F value low, while the other UO_2^{2+} ions which are free from the Cu^{2+} neighbors decay within their own relaxation mechanism.

The authors wish to express their thanks to Professor Kozo Nagashima for his kind support and encouragement during this work.

References

1) J. N. Demas and G. A. Crosby, *J. Phys. Chem.*, **75**, 991 (1971).
2) W. Lahmann and H. J. Ludewig, *Chem. Phys. Lett.*, **45**, 177 (1977).
3) M. J. Adams, J. G. Highfield, and G. F. Kirkbright, *Anal. Chem.*, **49**, 1850 (1977).
4) A. Rosencwaig, *Phys. Today*, **28**, 23 (1975).
5) K. Kato and Y. Sugitani, *Bull. Chem. Soc. Jpn.*, **52**, 3733 (1979).
6) K. Kato and Y. Sugitani, *Chem. Biomed. Environ. Instrumentation*, in press.
7) Y. Sugitani, H. Kasuya, K. Nagashima, and S. Fujiwara, *Nippon Kagaku Zasshi*, **90**, 52 (1969).
8) Y. Sugitani, K. Kato, and K. Nagashima, *Bull. Chem. Soc. Jpn.*, **52**, 918 (1979).
9) J. T. Bell and R. E. Biggers, *J. Mol. Spectrosc.*, **25**, 312 (1968).
10) E. Rabinowitch and R. L. Belford, "Spectroscopy and Photochemistry of Uranyl Compounds," Macmillan, New York (1964).
11) S. P. McGlynn and J. K. Smith, *J. Mol. Spectrosc.*, **6**, 164 (1961).
12) H. D. Burrows and T. J. Kemp, *Chem. Soc. Rev.*, **1974**, 139.
13) A. Rosencwaig and A. Gersho, *J. Appl. Phys.*, **47**, 64 (1976); E. M. Monahan, Jr. and A. W. Nolle, *ibid*, **48**, 3519 (1977).